Volume 257, number 2, 383–387 FEB 07803 November 1989

Differential allosteric effects of 8-(*N,N*-diethylamino)octyl-3,4,5-trimethoxybenzoate-HCl (TMB-8) on muscarinic receptor subtypes

Richard K. Gordon and Peter K. Chiang

Department of Applied Biochemistry, Walter Reed Army Institute of Research, Washington, DC 20307-5100, USA

Received 6 September 1989

TMB-8, a putative inhibitor of intracellular calcium mobilization, prevents the binding of the muscarinic ligand *N*-[^{3}H]methylscopolamine. The inhibition was observed in four tissues from guinea pig; cortex, heart, pancreas, and ileum, representing M1, cardiac M2, glandular M2, and heterogeneous M2 subtypes of muscarinic receptors, respectively. The K_i values for all four tissues were approx. 4 μM. However, dissociation kinetics revealed that TMB-8 interacted with an allosteric site of three muscarinic receptor subtypes but not the subtype from pancreas. These results indicate that TMB-8 interacts with muscarinic receptors, and therefore would disrupt calcium mobilization or any second messenger system coupled to these receptors.

Muscarinic receptor subtype; Allosteric site; Diethylamino octyl-3,4,5-trimethoxybenzoate-HCl 8-*N,N*-; Radioligand assay; Molecular model; Dissociation kinetics

1. INTRODUCTION

The mode of action of 8-(*N,N*-diethylamino)octyl-3,4,5-trimethoxybenzoate-HCl (TMB-8) has been attributed mainly to the inhibition of intracellular calcium mobilization, specifically preventing the release of calcium ions from the endoplasmic reticulum, but not Ca^{2+} influx [1,2]. In a number of related G-protein-coupled receptors, stimulation by an agonist leads to inositol phosphate metabolism and subsequently the release of Ca^{2+} from internal stores. TMB-8 has been widely used to characterize the role of Ca^{2+} in these second messenger systems [3]. However, TMB-8 has diverse and apparently contradictory effects, and TMB-8 has even been reported to mobilize rather than inhibit internal Ca^{2+} release in pancreatic beta cells [4].

The effect of TMB-8 on pancreatic tissue has been examined because pancreatic muscarinic receptors are coupled to the phosphatidylinositol-Ca^{2+} flux second messenger system [5]. Phosphatidylinositol metabolism and Ca^{2+} fluxes were inhibited by TMB-8, and a shift of the agonist dose response curve has been observed. These results suggest a competitive inhibition of the muscarinic response in pancreatic tissue by TMB-8 [6,7]. In addition, the binding of [^{3}H]quinuclidinyl benzylate to the pancreas muscarinic receptor was inhibited by TMB-8, although dose response and kinetic parameters were not reported [7]. Recently, TMB-8 has been shown to inhibit muscarinic receptor-mediated secondary events in adrenal chromaffin cells [8], adrenal glands [9], and cholinergic responses in cells containing cloned muscarinic receptor genes [10].

Whether TMB-8 competitively or allosterically interacts with muscarinic receptor subtypes remains to be determined. The existence of allosteric sites on muscarinic subtypes is reflected by changes in the dissociation of a radiolabeled antagonist bound to these receptors [11–13]. Thus, the effect of TMB-8 on binding parameters was examined here in four guinea pig tissues representing different muscarinic receptor subtypes: the cortex (M1), heart (cardiac M2), pancreas (glandular M2), and ileum (heterogeneous M2) [14–17].

2. MATERIALS AND METHODS

2.1. *Membrane preparations*

Male guinea pigs (200–400 g) were killed by decapitation and the brain, heart, pancreas, and ileum removed. Each tissue was minced in 20–30 vols of ice-cold buffer containing 50 mM potassium phosphate, pH 7.4, 80 μM EDTA, 100 μM phenylmethylsulfonyl fluoride and 0.32 M sucrose, and then homogenized. Each of the homogenates was centrifuged at 2500 × *g* for 15 min, resuspended in the buffer without sucrose, and centrifuged two additional times at 39000 × *g* for 20 min.

2.2. *Binding assays*

Equilibrium binding assays were performed as previously described [18,19]. Briefly, triplicate samples in the complete buffer were incubated with approx. 200 μg of protein and about 1 nM of *N*-[^{3}H]methylscopolamine ([^{3}H]NMS; 72 Ci/mmol, New England Nuclear, Boston, MA), yielding total counts between 2000 and 3000 dpm. Nonspecific binding was determined with 1 μM atropine and was about 100–300 dpm. TMB-8 (Sigma Chemical Co.,

Correspondence address: R.K. Gordon, Walter Reed Army Institute of Research, Department of Applied Biochemistry, Washington, DC 20307-5100, USA

Published by Elsevier Science Publishers B.V. (Biomedical Division)
00145793/89/$3.50

St.Louis, MO) was added with the [^{3}H]NMS. After 45 min at 25°C, the assays were terminated by collecting the samples on glass-fiber filters with a cell harvester and washing with cold complete buffer.

Specific binding was determined by subtracting the total from the nonspecific counts [18]. The IC_{50} values were calculated using LIGAND [20]. The K_i values were derived from the IC_{50} values by correcting for receptor occupancy [21] by the [^{3}H]NMS; the K_D values (nM) for the four different tissues were: cortex, 0.48; heart, 0.51; pancreas, 0.37; and ileum, 0.41.

2.3. *Dissociation kinetics assay*

The dissociation kinetics assay was performed by preincubating membranes containing muscarinic receptors with 1 nM [^{3}H]NMS for 90 min at 25°C. Subsequently, 1 μM atropine was added simultaneously with 0, 20, 50, or 100 μM TMB-8 for time intervals between 0.5 and 180 min; each assay was performed in triplicate.

The kinetic parameters of the dissociation curves were determined using the equation [11]: the [^{3}H]NMS bound to each tissue receptor (ligand-receptor complex) at a measured time (T) = $Ae^{-k_{-1}T} + Be^{-k_{-2}T}$. The portion of the bound ligand-receptor complex with a fast dissociating constant k_{-1} is denoted the 'A fraction'. B is the fraction with a slow dissociating constant k_{-2}. The parameters were fitted to curves using Gauss-Newton non-linear curve fitting programs (ASYSTANT, Macmillan Software Co., New York, NY) in double-precision mode. The regression coefficients for the curves were between 0.98 and 1.0. For Student's t-tests, a P value less than 0.05 was considered significant.

2.4. *Molecular modeling*

Molecular modeling of the protonated form of TMB-8 and atropine was performed as previously described [22]. Briefly, modeling was accomplished using XICAMM (XIRIS Corp., New Monmouth, NJ) computer programs. These algorithms are based on the classical molecular mechanical approach of Wipke et al. [23], and result in an energy-minimized, three-dimensional model of the molecule.

3. RESULTS

Fig.1 shows the inhibition of [^{3}H]NMS binding by TMB-8 in the membranes obtained from guinea pig cortex, heart, pancreas, and ileum, representing the muscarinic receptor subtypes M1, cardiac M2, glandular M2, and heterogeneous M2, respectively. The K_i ± SD values, determined from at least three dose-inhibition curves, were: cortex, 3.82 ± 0.21; ileum, 5.54 ± 0.91; pancreas, 4.24 ± 0.49; heart, 5.07 ± 0.88 μM. Hence, the K_i values were all approximately 4 μM, and were not significantly different from each other. The K_i values obtained from the inhibition curves of atropine in the cortex, heart, pancreas, and ileum membranes were 1.9, 1.4, 1.1, and 2.0 nM, respectively. Therefore, based on the binding data, atropine was about 2000-fold more potent a muscarinic antagonist than TMB-8. Next, the effect of TMB-8 on the dissociation kinetics of [^{3}H]NMS binding to the four different membranes was investigated. A decrease in the rate of dissociation of [^{3}H]NMS from muscarinic receptors would indicate an allosteric interaction by TMB-8.

The dissociation of bound [^{3}H]NMS in the presence of atropine alone or atropine and TMB-8 are shown in figs 2–5 for the cortex, heart, pancreas, and ileum membranes, respectively. The dissociation rate constants obtained from these figures by Gauss-Newton non-linear curve fitting programs are reported in table 1. The dissociation of the [^{3}H]NMS-receptor complex in the presence of atropine alone was biphasic in the membranes of cortex, ileum, and pancreas (table 1). In the heart membrane, the dissociation curve of [^{3}H]NMS in the presence of atropine was monophasic, and thus only one dissociation constant was obtained (table 1). The portion of muscarinic receptors possessing a fast dissociation constant is shown in table 1 under the heading, A fraction. A greater portion of the muscarinic receptor subtype in the ileum displayed a more rapid dissociation constant than in the cortex, while an even smaller portion was observed in the pancreas (0.76 vs 0.51 vs 0.14, respectively, table 1).

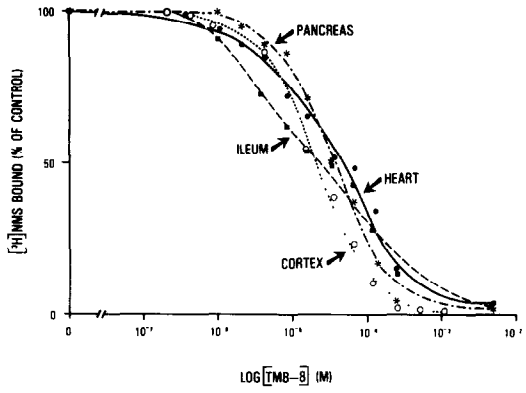

Fig.1. Displacement by TMB-8 of [^{3}H]NMS bound to the muscarinic receptors of guinea pig membranes obtained from the cortex (○---○), heart (●——●), pancreas (*---*), and ileum (■——■). Each point represents the mean of ≥3 experiments each in triplicate, and the SD values were less than 9%.

The dissociation curves obtained when 20–100 μM TMB-8 was added together with 1 μM atropine in the

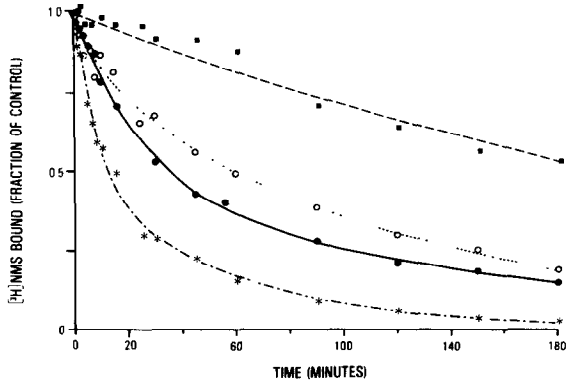

Fig.2. Dissociation curves obtained from cortex membranes. Time course of the dissociation of bound [^{3}H]NMS from the muscarinic receptors of the guinea pig membrane in the presence of the following drugs: 1 μM atropine alone (*---*); 1 μM atropine and 20 μM TMB-8 (●——●); 1 μM atropine and 50 μM TMB-8 (○---○); and 1 μM atropine and 100 μM TMB-8 (■- -■). Each point represents the mean of ≥3 experiments each in triplicate, and the SD values were less than 12%.

Table 1

Dissociation constants for [^{3}H]NMS binding to guinea pig muscarinic receptors

Tissue	Compound(s)	μM	Dissociation rate constants (min^{-1})		A fraction
			k_{-1}	k_{-2}	
Cortex	ATR		0.129 ± 0.004[a]	0.0176 ± 0.0008[a]	0.51 ± 0.01
	ATR + TMB-8	20	0.0405 ± 0.0020	0.00640 ± 0.00099	0.53 ± 0.07
	ATR + TMB-8	50	0.0744 ± 0.0042	0.00800 ± 0.00130	0.16 ± 0.01
	ATR + TMB-8	100	–	0.00337 ± 0.00092	–
Ileum	ATR		0.193 ± 0.027[a]	0.0147 ± 0.0028	0.76 ± 0.08
	ATR + TMB-8	20	–	0.0167 ± 0.0043	–
	ATR + TMB-8	50	–	0.00529 ± 0.00109	–
	ATR + TMB-8	100	–	0.00227 ± 0.00097	–
Pancreas	ATR		0.326 ± 0.024	0.0151 ± 0.0015	0.14 ± 0.02
	ATR + TMB-8	20	0.324 ± 0.029	0.0155 ± 0.0021	0.15 ± 0.02
	ATR + TMB-8	50	0.365 ± 0.022	0.0129 ± 0.0052	0.16 ± 0.02
	ATR + TMB-8	100	0.308 ± 0.019	0.0122 ± 0.0014	0.18 ± 0.02
Heart	ATR		–	0.137 ± 0.023[a]	–
	ATR + TMB-8	20	–	0.0208 ± 0.0065	–
	ATR + TMB-8	50	–	0.00383 ± 0.00054	–
	ATR + TMB-8	100	–	0.000669 ± 0.000094	–

[a] Significantly different compared to the corresponding dissociation constant in the presence of TMB-8

(–) Monophasic kinetics rather than biphasic. After 90 min incubation with 1 nM [^{3}H]NMS, 1 μM atropine (ATR) was added to each sample along with the indicated concentration of TMB-8, 0–100 μM. The mean ± SD are listed for ≥3 experiments, each in triplicate. The dissociation constants were determined as described in section 2, using the equation [11]: [^{3}H]NMS bound to each tissue (ligand-receptor complex) at a measured time (T) = $Ae^{-k_{-1}T} + Be^{-k_{-2}T}$. The portion of bound ligand-receptor complex with a fast dissociating constant k_{-1} is denoted the 'A fraction'; B is the fraction with a slow dissociating constant k_{-2} (i.e., $1 - A = B$)

pancreas membrane were similar (fig.4), and there was no significant difference between the dissociation rate constants derived from these curves (table 1). In contrast to the results obtained with the pancreas membrane, higher concentrations of TMB-8 resulted in upward shifts of the cortex, heart, and ileum dissociations curves, corresponding to a decrease in the dissociation rate constants (table 1, figs 2,3,5). However, the shifts in the curves were not identical for all muscarinic receptor subtypes. The addition of 20 μM TMB-8 together with 1 μM atropine significantly decreased both the k_{-1} and k_{-2} dissociation constants in the cortex and ileum membranes compared to atropine alone (table 1, and figs 2,5). When TMB-8 was present at 20 μM in the ileum assay or 100 μM in the cortex assay, the k_{-1} rate constant disappeared so that only a single slow rate constant k_{-2} was observed in these membranes. If the fast component of dissociation was eliminated, TMB-8 continued to reduce the slow component, k_{-2}, at higher concentrations. In the heart membrane, where only a monophasic kinetics constant was obtained with 1 μM atropine, TMB-8 decreased this rate constant in a dose-dependent manner (fig.3).

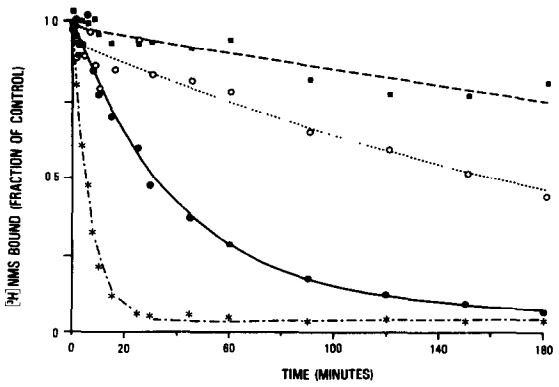

Fig.3. Dissociation curves obtained from heart membrane; same symbols and legend as fig.2.

4. DISCUSSION

TMB-8 has been shown to inhibit competitively the pharmacological responses of pancreas slices to the muscarinic agonist carbachol [6,7]. These observations were further extended by the present study with the pancreas muscarinic receptor. First, TMB-8 inhibited [^{3}H]NMS binding to the pancreas muscarinic receptor in a dose-dependent manner (fig.1), and did not alter either the k_{-1} or k_{-2} dissociation rate constants (fig.4, table 1). Hence, TMB-8 did not modulate allosterically

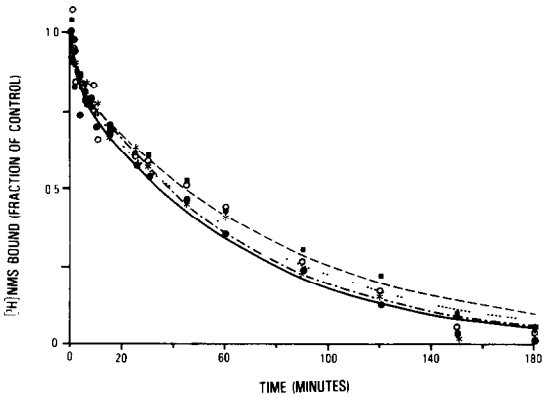

Fig.4. Dissociation curves obtained from pancreas membrane; same symbols and legend as fig.2.

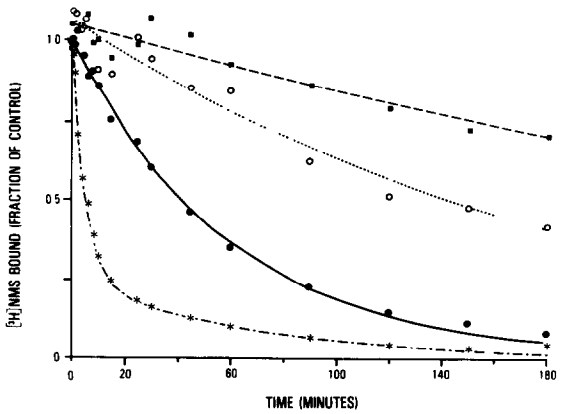

Fig.5. Dissociation curves obtained from ileum membrane; same symbols and legend as fig.2.

[^{3}H]NMS binding in the pancreas. These and previous results [22] indicate that the pancreas muscarinic receptor subtype is different from the ileum subtype.

In contrast to the results observed with the pancreas tissue, TMB-8 demonstrated allosteric inhibition of the dissociation curves of bound [^{3}H]NMS from muscarinic receptor subtypes in cortex, ileum, and heart membranes. The allosteric interaction of TMB-8 was clearly demonstrated in figs 2,3 and 5 by the upward shift of the dissociation curves [11–13] with increasing concentrations of TMB-8, corresponding to a decrease in the dissociation rate constants (table 1). Thus, TMB-8 stabilized the [^{3}H]NMS-receptor complex in these membranes.

The differential effect of TMB-8 only on the dissociation kinetics of [^{3}H]NMS from the muscarinic receptor subtypes (table 1), and not on the inhibition constants ($K_i \cong 4\ \mu M$ in all four membranes), indicated that TMB-8 was not a selective agent for the antagonist-binding site of the subtypes. Rather, TMB-8 was selective for allosteric site(s) of the muscarinic receptors, and is unlike the receptor selectivity of subtype specific ligands such as pirenzepine or AF-DX 116, which are directed towards the M1 and M2 antagonist-binding sites, respectively [14–17].

The computer generated models of TMB-8 and atropine were energy-minimized and then superimposed (fig.6). Two important functional groups, the ester and the bulky hydrophobic groups, could be overlayed in close proximity, while the protonated nitrogen group in TMB-8 was more distant from the carbonyl oxygen of the ester group than observed for atropine, 7.0 Å compared to 4.9 Å, respectively. An optimum geometric distance of 5.1–5.2 Å between the protonated nitrogen and the carbonyl oxygen has been determined for antagonists [22,24]. The increased distance could be responsible partially for the 2000-fold reduced potency of TMB-8 compared to atropine. Additionally and unlike atropine, TMB-8 has a flexible eight-carbon aliphatic chain between the ester and the protonated nitrogen, which would permit other low energy conformations where the TMB-8 nitrogen does not correspond to the location of the atropine nitrogen. These alternative TMB-8 conformations might bind to an allosteric site in the receptor subtypes of the cortex, heart, and ileum. Based on the different dissociation kinetics observed for each membrane, the allosteric sites were probably not identical in each receptor subtype, and the pancreas receptor subtype lacked an allosteric site. The flexibility or rigidity of an antagonist has been proposed as a mechanism by which a compound can attain the conformation necessary to interact with subtypes of muscarinic receptors [25].

Typical doses of TMB-8 used to block internal calcium mobilization range from 10 to 200 μM [4]. The IC_{50} values for TMB-8 inhibition of the four muscarinic receptor subtypes examined in this report were approx. 20 μM (fig.1), or K_i values of about 4 μM. These values are well within the dose of TMB-8 which affects pharmacological responses of the pancreas; the extrapolated IC_{50} values derived from the curves in [6] were about 50 μM for inhibiting α-amylase release or inhibiting the initial rise in internal Ca^{2+}. Since TMB-8 can act directly at the receptor, both competitively and allosterically, it would be expected that calcium mobilization induced by muscarinic receptor stimulation, or any second messenger system coupled to the muscarinic receptors, to be inhibited by TMB-8.

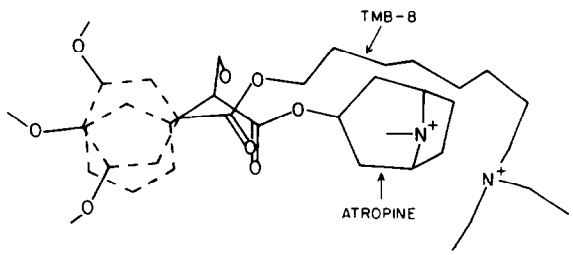

Fig.6. Modeled structures of TMB-8 and atropine, which have been energy-minimized and then superimposed. The structures were then compared by minimizing the distance between three groups important for potency at the muscarinic receptor (see section 4; [22,24]).

REFERENCES

[1] Malagadi, M.H. and Chiou, C.Y. (1974) Eur. J. Pharmacol. 27, 25–33.

[2] Chiou, C.Y. and Malagodi, M.H. (1985) Br. J. Pharmacol. 53, 279–285.

[3] Brand, M.D. and Felber, S.M. (1984) Biochem. J. 224, 1027–1030.

[4] Pian-Smith, M.C., Yada, T., Yaney, G.C., Abdel el Motal, S.M., Wiedenkeller, J.D.E. and Sharp, G.W.G. (1988) Endocrinology 123, 1984–1991.

[5] Streb, H., Heslop, J.P., Irvine, R.F., Schulz, I. and Berridge, M.J. (1985) J. Biol. Chem. 260, 7309–7315.

[6] Willems, P.H.G.M., Van Nooig, I.G.P. and De Pont, J.J.H.H.M. (1986) Biochim. Biophys. Acta 888, 255–262.

[7] Tennes, K.A., Kennedy, J.A. and Roberts, M.L. (1983) Biochem. Pharmacol. 32, 2116–2118.

[8] Misbahuddin, M. and Oka, M. (1988) Neurosci. Lett. 87, 266–270.

[9] Yamada, Y., Teraoka, H., Nakazato, Y. and Ohga, A. (1988) Neurosci. Lett. 90, 338–342.

[10] Conklin, B.R., Brann, M.R., Buckley, N.J., Ma, A.L., Bonner, T.I. and Axelrod, J. (1988) Proc. Natl. Acad. Sci. USA 85, 8698–8702.

[11] Narayanan, T.K. and Aronstam, R.S. (1986) Neurochem. Res. 11, 1397–1406.

[12] Waelbroeck, M., De Neef, P., Robberecht, P. and Christophe, J. (1984) Life Sci. 35, 1069–1076.

[13] Nedoma, J., Tucek, S., Danilov, A.F. and Shelkovnikov, S.A. (1986) J. Pharmacol. Exptl. Ther. 236, 219–223.

[14] Giraldo, E., Alessandra Vigano, M., Hammer, R. and Ladinsky, H. (1988) Mol. Pharmacol. 33, 617–625.

[15] Peralta, E.G., Winslow, J.W., Peterson, G.L., Smith, D.H., Ashkenazi, J., Ramachandran, J., Schimerlik, M.I. and Capon, D.J. (1987) Science 236, 600–605.

[16] Buckley, N.J., Bonner, T.I., Buckley, C.M. and Brann, M.R. (1989) Mol. Pharmacol. 35, 469–476.

[17] Doods, H.N., Mathy, M.-J., Davidesko, D., Van Charldorp, K.J., De Jonge, A. and Van Zwieten, P.A. (1987) J. Pharmacol. Exp. Ther. 242, 257–262.

[18] Ahmad, A., Gordon, R.K. and Chiang, P.K. (1987) FEBS Lett. 214, 285–290.

[19] Gordon, R.K. and Chiang, P.K. (1986) J. Pharmacol. Exp. Ther. 236, 85–89.

[20] Munson, P.J. and Rodbard, D. (1979) Endocrinology 105, 1377–1381.

[21] Cheng, Y.-C. and Prusoff, W.H. (1973) Biochem. Pharmacol. 22, 3099–3108.

[22] Gordon, R.K., Breuer, E., Padilla, F.N., Smejkal, R.M. and Chiang, P.K. (1989) Mol. Pharmacol., in press.

[23] Wipke, W.T. and Dyott, T.M. (1974) J. Am. Chem. Soc. 96, 4825–4834.

[24] Schulman, J.M., Sabio, M.L. and Disch, R.L. (1983) J. Med. Chem. 26, 817–823.

[25] Messer, W.S., jr, Ellerbrock, B.R., Smith, D.A. and Hoss, W. (1989) J. Med. Chem. 32, 1164–1172.